Available online at www.sciencedirect.com
ScienceDirect
Journal of Solid State Chemistry 181 (2008) 646–651
JOURNAL OF SOLID STATE CHEMISTRY
www.elsevier.com/locate/jssc

# A new promising scintillator $Ba_3InB_9O_{18}$

Gemei Cai[a], X.L. Chen[a,*], W.Y. Wang[a], Y.F. Lou[a,b], J. Liu[a], J.T. Zhao[c], H.H. Chen[c]

[a]*Beijing National Laboratory for Condensed Matter Physics, Institute of Physics, Chinese Academy of Sciences, P.O. Box 603, Beijing 100080, PR China*
[b]*Center of Condensed Matter and Materials Physics, School of Sciences, Beihang University, Beijing 100083, PR China*
[c]*Ceramics and Superfine Microstructure, Shanghai Institute of Ceramics, Chinese Academy of Sciences, Shanghai 200050, PR China*

Received 25 October 2007; received in revised form 19 December 2007; accepted 27 December 2007
Available online 2 January 2008

**Abstract**

We report on the synthesis, crystal structure and scintillation property of a new compound $Ba_3InB_9O_{18}$. This compound crystallizes in space group $P6_3/m$ with unit cell of dimensions $a = 7.1359(3)$ Å, $c = 16.6151(8)$ Å and $V = 732.697$ Å$^3$ with two $Ba_3InB_9O_{18}$ molecular formula. Its crystal structure is made up of planar $B_3O_6$ groups parallel to each other along the $\langle 0001 \rangle$ direction, regular $InO_6$ octahedra, irregular $BaO_6$ hexagons and $BaO_9$ polyhedra to form an analog structure of $Ba_3YB_9O_{18}$. DTA and TGA curves for $Ba_3InB_9O_{18}$ show that it is a chemically stable and congruent melting compound. Its X-ray excited luminescence spectra show an intense emission band in the range of 360–500 nm with a maximum at 400 nm. Light yield for $Ba_3InB_9O_{18}$ is about 75% as large as that for BGO under the same measurement conditions. There may exist a correlation between the scintillation properties and the crystal structural features of $Ba_3InB_9O_{18}$.


*Keywords:* Borate; Crystal structure; Powder diffraction; Rietveld refinement; Luminescence; Scintillation

## 1. Introduction

The development of high-energy physics, irradiation medicine, geology prospecting, safety scanning, petroleum exploration and so on, determines the necessity of search for new detectors, specifically, scintillation materials. High light yield (LY), low decay time and strong stopping power, are among the most desired properties of scintillators. Nowadays, one of commercial scintillation crystals is $Bi_4Ge_3O_{12}$ (BGO) because of its high LY (3420 p.e./MeV), though its decay time is a little long (300 ns) [1]. A traditional scintillation crystal $PbWO_4$ [2] finds intensive applications for electromagnetic calorimeters and photon detectors in high-energy physics due to its very fast decay (10 ns). Meanwhile, researchers have been trying to increase its LY by doping to meet the requirements for detecting efficiently low-energy particles [3,4]. Subsequently, scintillation crystals of fluoride, doped silicates, Lu-containing perovskites and garnets, are widely developed and exhibit higher LYs and shorter decay times. Examples include $CeF_3$, $Gd_2SiO_5$:Ce (GSO), $Lu_2SiO_5$:Ce (LSO), $LuAlO_3$ (LuAP) and $Lu_3Al_5O_{12}$:Yb (LuAG) and so on [5–10]. However, the difficulty in crystal growth due to high melting points and comparably high cost are not favorable for future commercial applications of these crystals.

Borates have taken a special place among functional materials due to their rich varieties in crystal structure [11–13], wide transmittance spectra with high damage threshold, and wide band gaps. Much effort has been focused on the synthesis, crystal growth and characterization of inorganic borates with potential applications as optical materials, for instance, materials for second harmonic generation (SHG) or host materials for luminescence [14–16]. As a part of a project for search for new functional materials, our group has investigated several ternary systems of borates [17–20]. Recently, a systematic survey of the $BaO–Y_2O_3–B_2O_3$ system has led to the discovery of a series of new isostructural borates $Ba_3MB_9O_{18}$ ($M$ = Y, Pr, Nd, Sm–Yb) [20]. Subsequently, He et al. [21] grew the single crystal $Ba_3YB_9O_{18}$ and reported

*Corresponding author. Fax: +86 10 8264 9646.
*E-mail address:* chenx29@aphy.iphy.ac.cn (X.L. Chen).

0022-4596/$ - see front matter © 2007 Elsevier Inc. All rights reserved.
doi:10.1016/j.jssc.2007.12.030

its interesting scintillation properties. Very recently, a scandium substituted derivative $Ba_3ScB_9O_{18}$ with better scintillation property was obtained [22]. As is well-known, binary indium borate $InBO_3$ [23] is of interest for its rare-earth-doped luminescence properties [24,25]. However, very few studies on $MO$–$In_2O_3$–$B_2O_3$ ($M$ = Ca, Sr, Ba) systems has been carried out by far. Only a handful of ternary indium borates have been reported: $Li_3In_2B_3O_9$ [26], $Sr_2LiInB_4O_{10}$ [27], and $Li_3InB_2O_6$ [28]. To explore new scintillation materials, we have undertaken a systematic survey of the $BaO$–$In_2O_3$–$B_2O_3$ system by means of solid-state reactions. A new indium borate $Ba_3InB_9O_{18}$ has been identified. In this paper, we will present the results on the synthesis, crystal structure, and excellent scintillation characteristics of $Ba_3InB_9O_{18}$.

## 2. Experimental

### 2.1. Synthesis, chemical analysis and X-ray powder diffraction

A powder sample of the title compound was prepared by the high-temperature solid-state technique. A stoichiometric mixture of $BaCO_3$ (spectral reagent), $In_2O_3$ (analytical reagent), and $H_3BO_3$ (analytical reagent) were finely ground into powders in a mortar of agate. The mixture was preheated in a platinum crucible for 12 h at 650 °C to decompose $H_3BO_3$ and $BaCO_3$. They were reground and sintered at 920 °C for 72 h with an intermediate grinding. In all cases, care was taken to add extra 1 mol% $H_3BO_3$ in order to offset the weight losses of $B_2O_3$ in the procedure of synthesis.

The atomic ratio of In, Ba and B in the sample were near to 1:3:9, measured by inductively coupled plasma atomic emission spectrometry using a Perkin Elmer ICP/6500 spectrometer.

X-ray powder diffraction data were recorded on an X-ray diffractometer (MXP21VAHF/M21X, MAC Science) with Cu$K\alpha$ radiation and a diffracted-beam graphite monochromator operated at a power of 50 kV and 200 mA. No peaks attributable to impurity were identified in the powder XRD pattern. The data for crystal structure analysis were collected at room temperature in step scan mode with a step size 0.02° ($2\theta$), counting time 3 s per step and $2\theta$ range of 10–130°. More technical details were listed in Table 1.

### 2.2. Structure determination and refinement

All the reflections of new compound $Ba_3InB_9O_{18}$ can be indexed on the basis of a hexagonal unit cell with lattice parameters $a = 7.1361(4)$ Å and $c = 16.608(1)$ Å using the program DICVOL04 [29]. The systematic absences ($000l$: $l = 2n+1$) are consistent with space group $P6_3$ and $P6_3/m$. Comparisons between $Ba_3InB_9O_{18}$ and $Ba_3YB_9O_{18}$ in crystal system, lattice parameters and powder XRD pattern, show that the two compounds are isostructural. So we choose the space group $P6_3/m$. In addition, there is no efficiency of SHG in powder samples of $Ba_3InB_9O_{18}$ using the Kurtz–Perry technique [30], which suggests centrosymmetric $P6_3/m$ space group is more probable.

Table 1
Details of Rietveld refinement and crystal data of $Ba_3InB_9O_{18}$

| | |
|---|---|
| Sample | Multi-crystal powder |
| Diffractometer | MXP21VAHF/M21X |
| Radiation type | Cu$K\alpha$ |
| Monochromator | Graphite |
| Wavelength (Å) | 1.5405 |
| Refined profile range (°$2\theta$) | 10–130 |
| Step size (°$2\theta$) | 0.02 |
| Step scan time per step (s) | 3 |
| Number of structure parameters | 32 |
| Number of profile parameters | 13 |
| $R_B$ | 4.76% |
| $R_P$ | 7.55% |
| $R_{WP}$ | 9.69% |
| $S$ | 1.76 |
| Formula | $Ba_3InB_9O_{18}$ |
| Symmetry | Hexagonal |
| Space group | $P6_3/m$ |
| $a$ (Å) | 7.1359(3) |
| $c$ (Å) | 16.6151(8) |
| Volume (Å$^3$) | 732.697 |
| $Z$ | 2 |
| Measured density (g cm$^{-3}$) | 4.145 |
| Calculated density (g cm$^{-3}$) | 4.134 |

According to the structural model of $Ba_3YB_9O_{18}$, we refined the structure parameters of $Ba_3InB_9O_{18}$ from the powder XRD data by the Rietveld method [31] using the program FullProf_suite [32]. The profile range of data used for refinement was 10–130° in $2\theta$. A total of 32 structural parameters and 13 profile parameters were refined. The refinement finally converged to agreement factors of $R_B = 4.76\%$, $R_P = 7.55\%$ and $R_{WP} = 9.69\%$ with $S = 1.76$. The final refinement pattern is shown in Fig. 1. Details of Rietveld refinement and crystal data are given in Table 1. Positional parameters obtained by the Rietveld refinement are listed in Table 2. The bond lengths ($r$), $\delta$ values ($\delta = (d-r)/d$, where the $d$ is the sum of the respective atomic radii) and some selected geometric parameters in the hexagonal structure of $Ba_3InB_9O_{18}$ are listed in Table 3.

### 2.3. IR spectra measurement

Infrared spectra in the 350–2000 cm$^{-1}$ wave number range were obtained by using a Perkin-Elmer 983G infrared spectrophotometer with KBr pellets as standards.

### 2.4. Differential thermal analysis

The thermal stability was investigated by differential thermal analysis. A CP-G high-temperature differential thermal instrument was employed to perform DTA and TGA. Sample and alumina reference were enclosed in

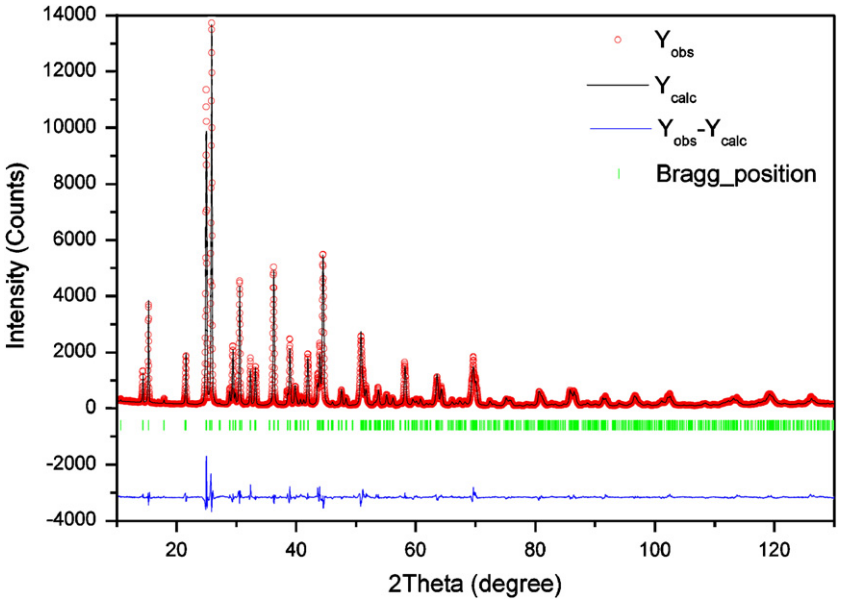


Fig. 1. Final Rietveld refinement patterns of $Ba_3InB_9O_{18}$.

Table 2
Atomic coordinates and isotropic displacement parameters for $Ba_3InB_9O_{18}$

| Atom | Site | *X* | *y* | *z* | B (Å$^2$) |
|---|---|---|---|---|---|
| Ba1 | 4*f* | 1/3 | 2/3 | 0.12864(3) | 0.486(6) |
| In | 2*b* | 0 | 0 | 0 | 0.93(1) |
| Ba2 | 2*a* | 0 | 0 | 1/4 | 1.30(2) |
| O1 | 6*h* | 0.451(1) | 0.294(1) | 1/4 | 0.59(6) |
| O2 | 12*i* | −0.1029(7) | 0.3956(7) | 0.0786(2) | 1.01(5) |
| O3 | 6*h* | 0.5988(8) | 0.6692(8) | 1/4 | 0.67(5) |
| O4 | 12*i* | −0.0092(5) | 0.7515(5) | 0.0791(2) | 0.74(5) |
| B1 | 6*h* | 0.632(2) | 0.493(2) | 1/4 | 1.5(1) |
| B2 | 12*i* | −0.179(1) | 0.540(1) | 0.0780(4) | 0.47(7) |

$Al_2O_3$ cups. The heating rate was 10 °C/min in a temperature range from room temperature to 1150 °C.

### 2.5. XEL measurement

Scintillation property was studied by X-ray excited luminescence spectra. XEL spectra for the compound were measured at room temperature using an X-ray excited spectrometer (Fluormain) in which an F-30 X-ray tube (*W* anticathode target) was used as an X-ray source.

## 3. Results and discussion

### 3.1. Crystal structure

The structure of $Ba_3InB_9O_{18}$ is depicted in Fig. 2. The oxygen polyhedron of one independent In site is a regular octahedron ($InO_6$), at equal bond distances of 2.1817 Å comparable to In–O bond lengths of 2.18 Å in $In_2O_3$ [33], 2.17 Å in $Li_3InB_2O_6$ [28] and 2.17 Å calculated with crystal radii for a hexa-coordinated In atom. Six vertexes of each $InO_6$ octahedron interconnect six planar $B_3O_6$ rings, and three vertexes of each planar $B_3O_6$ ring interconnect three $InO_6$ octahedra.

The Ba(1) atom is bound to six O atoms at length ranging from 2.7605 to 2.9152 Å with average Ba(1)–O distance, 2.841 Å, comparable to the value 2.8 Å reported in $Ba_3M(BO_3)_3$ ($M$ = Dy, Ho, Y, Er, Tm, Yb, Lu, and Sc) [34]. The Ba(2) atoms occupy nine-vertex polyhedra having distorted, parallel hexagonal, and trigonal bases. In this

Table 3
Selected geometric parameters (Å or °)

| Atom | *r* | δ(%) | Atom | *r* | δ(%) |
|---|---|---|---|---|---|
| Ba(1)–O(3)$_{i}$ | 2.7605 | 2.80 | Ba(2)–O(3)$_{ii}$ | 2.6477 | 6.77 |
| Ba(1)–O(3)$_{ii}$ | 2.7605 | 2.80 | Ba(2)–O(3)$_{v}$ | 2.6477 | 6.77 |
| Ba(1)–O(3) | 2.7606 | 2.80 | Ba(2)–O(3)$_{vi}$ | 2.6477 | 6.77 |
| Ba(1)–O(2)$_{ii}$ | 2.8463 | −0.22 | Ba(2)–O(1)$_{viii}$ | 2.8297 | 0.36 |
| Ba(1)–O(2) | 2.8463 | −0.22 | Ba(2)–O(1)$_{vii}$ | 2.8297 | 0.36 |
| Ba(1)–O(2)$_{i}$ | 2.8464 | −0.22 | Ba(2)–O(1) | 2.8297 | 0.36 |
| Ba(1)–O(4) | 2.9151 | −2.64 | Ba(2)–O(4) × 6 | 3.3310 | −14.74 |
| Ba(1)–O(4)$_{ii}$ | 2.9152 | −2.64 | In(1)–O(4)$_{ix}$ | 2.1817 | 3.46 |
| Ba(1)–O(4)$_{i}$ | 2.9152 | −2.64 | In(1)–O(4)$_{x}$ | 2.1817 | 3.46 |
| B(1)–O(1)$_{iii}$ | 1.3509 | 9.94 | In(1)–O(4)$_{xi}$ | 2.1817 | 3.46 |
| B(1)–O(1) | 1.3604 | 9.31 | In(1)–O(4)$_{xii}$ | 2.1817 | 3.46 |
| B(1)–O(3)$_{i}$ | 1.3910 | 7.27 | In(1)–O(4)$_{xiii}$ | 2.1817 | 3.46 |
| B(2)–O(2)$_{i}$ | 1.3843 | 7.71 | In(1)–O(4)$_{i}$ | 2.1817 | 3.46 |
| B(2)–O(4) | 1.3848 | 7.68 | | | |
| B(2)–O(2)$_{iv}$ | 1.4283 | 4.78 | | | |
| O(1)$_{iii}$–B(1)–O(3) | 113.639 | 5.30 | O(2)–B(2)–O(2)$_{iv}$ | 130.265 | −8.55 |
| O(1)–B(1)–O(3) | 116.208 | 3.16 | O(2)$_{iv}$–B(2)–O(4) | 118.854 | 0.96 |
| O(1)$_{iii}$–B(1)–O(1) | 130.153 | −8.46 | O(2)–B(2)–O(4) | 110.857 | 7.62 |

(i) $1-y,1+x-y,\ z$; (ii) $-x+y,\ 1-x,\ z$; (iii) $1-x+y,\ 1-x,\ z$; (iv) $-y,\ 1+x-y,\ z$; (v) $1-y,\ x-y,\ z$; (vi) $-1+x,-1+y,\ z$; (vii) $-x+y,\ -x,\ z$; (viii) $-y,\ x-y,\ z$; (ix) $-1-x+y,\ -x,\ z$; (x) $-x,\ 1-y,\ -z$; (xi) $-1+y,\ -1-x+y,\ -z$; (xii) $1+x-y,\ x,\ -z$; (xiii) $x,\ -1+y,\ z$.

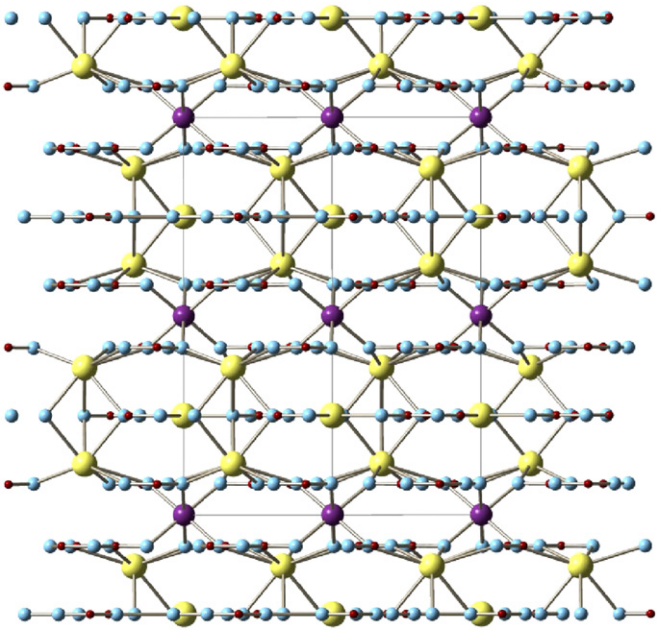

Fig. 2. Structure of $Ba_3InB_9O_{18}$ along the ⟨11–20⟩ direction.

environment, each Ba(2) atom binds six O atoms at the vertices of a distorted hexagon in one plane and three additional O atoms in a subjacent plane. The average Ba(2)–O distance, 2.739 Å, agrees well with the value of 2.749 Å in $\beta$-$Ba_3YB_3O_9$ [35].

In the building units of $Ba_3InB_9O_{18}$ structure, B(1) species are coordinated to O(1) and O(3) to form $B_3O_6$ rings. The three vertexes O(3) of a $B_3O_6$ ring are shared by one Ba(2)$O_6$ and two Ba(1)$O_9$, and the three O(1) at the edge of $B_3O_6$ ring are common with three planar Ba(2)$O_6$. Three B(2) with three O(2) and three O(4) atoms form $B_3O_6$ rings which interconnect In$O(4)_6$ octahedra and irregular Ba(1)$O_9$ polyhedra parallel to the *ab* crystal plane. The planar $B_3O_6$ rings are parallel to each other and stack layer upon layer along the *c* axis.

All standard deviations ($\delta$ values) for bond lengths and angles are smaller than 15% and within experimental error of those values expected for metrically regular geometries.

To examine the validity of the determined structure of $Ba_3InB_9O_{18}$, Brown's bond valence theory [36] was used to calculate the valence sum for each ion. From the results of the calculations given in Table 4, we can see that the calculated valence sums for all ions are reasonable.

### 3.2. *IR Spectra for* $Ba_3MB_9O_{18}$

In order to further confirm the coordination surroundings of B–O in the $Ba_3InB_9O_{18}$ structure, an infrared absorption spectrum for $Ba_3InB_9O_{18}$ was measured at room temperature and given in Fig. 3. Bands below 400 $cm^{-1}$ should be due to crystal lattice vibrations. The absorption wave number profile in 428, 511, and 600–800 $cm^{-1}$ is assigned to bending vibration of In–O bonds, Ba–O bonds and $BO_3$ units, respectively. The

Table 4
Bond valence analysis of $Ba_3InB_9O_{18}$

| Atoms | O(1) | O(2) | O(3) | O(4) | $\Sigma s_{calc}$ | $\Sigma s_{theo}$ |
|---|---|---|---|---|---|---|
| Ba(1) | | 0.22034 × 3 | 0.27826 × 3 | 0.118224 × 3 | 2.042 | 2 |
| Ba(2) | 0.2306 × 3 | | 0.37409 × 3 | 0.06067 × 6 | 2.178 | 2 |
| In(1) | | | | 0.46957 × 6 | 2.817 | 3 |
| B(1) | 1.05298 | | 0.94853 | | 3.008 | 3 |
| | 1.02625 | | | | | |
| B(2) | | 0.96422 | | 0.96302 | 2.804 | |
| | | 0.87687 | | | | 3 |

*Note*: The results refer to the equation $s = \exp[(r_0 - r)/B]$ with $r_0 = 2.285$, 1.902 and 1.371 Å for Ba–O, In–O and B–O, respectively, and $B = 0.37$.

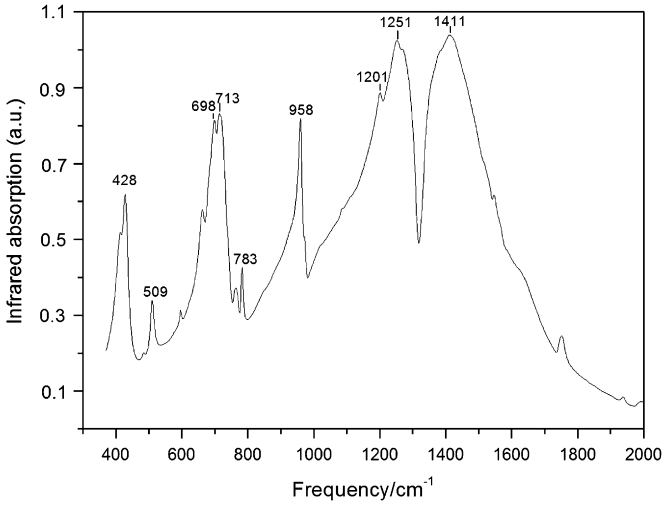


Fig. 3. Infrared spectra for $Ba_3InB_9O_{18}$.

absorption at wave number 958 $cm^{-1}$ originates mainly from the B–O asymmetric stretching of $B_3O_6$ groups. According to previous work [37], the strong bands above 1145 $cm^{-1}$ are generated by the stretching vibrations of the triangular $BO_3$ groups.

### 3.3. *Occurrence of borate* $Ba_3MB_9O_{18}$

The compound $Ba_3InB_9O_{18}$ belongs to a large family of synthetic borates, having the formula $Ba_3MB_9O_{18}$ ($M$ = Sc, Y, Pr–Yb, In). These materials adopt a layered-type structure which contains discrete planar hexagonal $[B_3O_6]^{3-}$ rings that stack parallel or antiparallel to each other along the *c*-axis. These layers connected with deformed $BaO_6$ hexagons are interleaved with regular $MO_6$ octahedra and irregular $BaO_9$ polyhedra. In this environment, each $M$ ion bonds to six separate $BO_3$ groups, i.e., forming octahedral $M(BO_3)_6$.

Syntheses of other substituted derivatives were attempted after $Ba_3InB_9O_{18}$. However, the attempted solid-state syntheses of the following compounds were unsuccessful: $A_3MB_9O_{18}$ ($A$ = Ca, Sr, and $M$ = Sc, Y, Pr–Yb, In, Bi). Either melting occurred at low temperature or other more stable borates formed. For instance, in the

case of $Sr_3EuB_9O_{18}$, the only crystalline products were $EuBO_3$, $SrB_2O_4$ and $SrB_4O_7$. It is suggested that a certain factor may be dominant in determining their stabilities. Substituting the $Y^{3+}$ ions in $Ba_3YB_9O_{18}$ with $La^{3+}$ was a failure. The reason is probably that the ionic radius of $La^{3+}$ is too large. The ion radius of $La^{3+}$ seems to exceed the upper limit for the stabilization zone of this structure-type. In any case, we can conclude that the $Ba_3MB_9O_{18}$ crystal structure can well accommodate a large range of trivalent $M$ cations whose ion radii are between 0.75 and 1.13 Å. The possible existence of the Bi derivative remains to be investigated.

### 3.4. Thermal stability

Fig. 4 presents the DTA and TGA curves for $Ba_3InB_9O_{18}$. No weight loss was detected from room temperature to 1150 °C. The endothermic peak at about 1000 °C should be the melting point for the compound $Ba_3InB_9O_{18}$. The DTA and TGA curves for $Ba_3InB_9O_{18}$ show that it is a chemically stable and congruent melting compound.

### 3.5. Scintillation characteristics

XEL measurements were performed on polycrystalline $Ba_3InB_9O_{18}$ and BGO samples at room temperature. Fig. 5 shows a comparison between the XEL spectrum of BGO and $Ba_3InB_9O_{18}$ under the same measurement conditions. $Ba_3InB_9O_{18}$ exhibited a broad and intense emission band in the range of 360–500 nm with maximum at 400 nm. Such a XEL feature for $Ba_3InB_9O_{18}$ is similar to that of $Ba_3YB_9O_{18}$, $Ba_3Lu(BO_3)_3$, and $\alpha$-$Ba_3Y(BO_3)_3$ reported in previous researches [21,35]. Comparing the integral area of the emission bands for the title compound with that for BGO, it is interesting to notice that the LY of $Ba_3InB_9O_{18}$ is about 75% as large as that of BGO. As far as the scintillation mechanism is concerned, there may be an important correlation between their efficient XEL and the

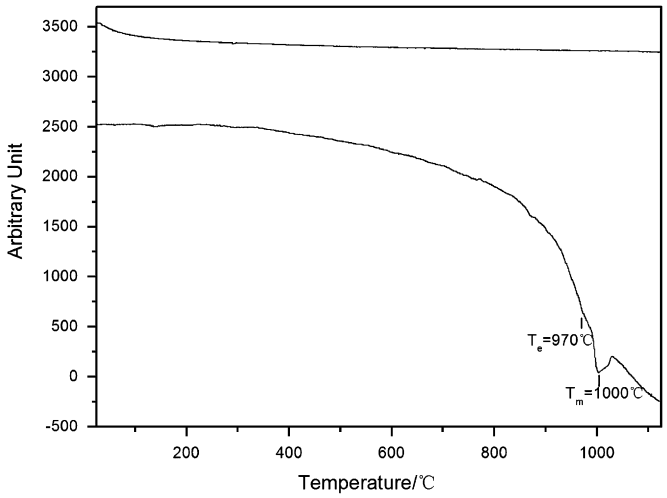


Fig. 4. DTA and TGA curves for $Ba_3InB_9O_{18}$.

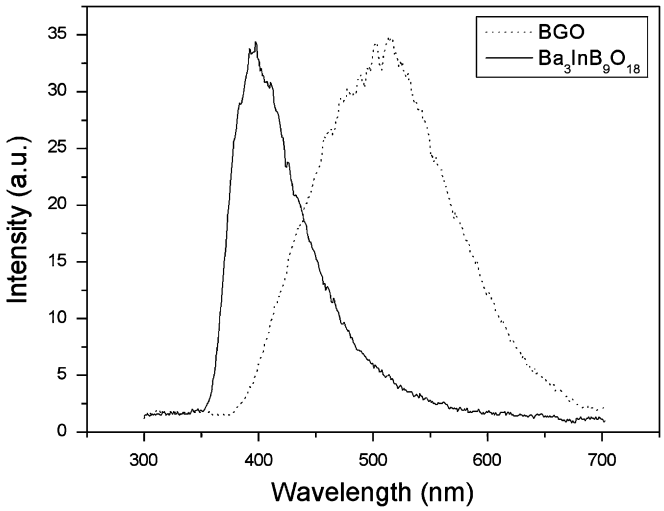


Fig. 5. Comparison of the XEL spectra for polycrystalline BGO and $Ba_3InB_9O_{18}$ under the same measurement conditions.

structural features for this type of compounds. Lattice defects such as oxygen vacancies, excess negative charges and excitons, probably play an important role on the scintillating properties of these materials, as reported in literature [38]. A detailed study of the scintillation mechanism will be useful. Previous research results show that the decay time for $Ba_3YB_9O_{18}$ is 27 ns [38]. It is speculated that the decay time for isostructural $Ba_3InB_9O_{18}$ is similar.

High LY and fast decay can compensate the possible disadvantage of comparably low density of $Ba_3InB_9O_{18}$ (4.133 g/cm$^3$). In addition, the polycrystalline $Ba_3InB_9O_{18}$ is highly stable in air and neither hygroscopic nor soluble in water. Therefore, we can conclude that the title compound can be a promising scintillator for X-radiation. The neutron detection ability has not been known for $Ba_3InB_9O_{18}$. However, this compound may not be suitable for the detector in neutron applications because $^{10}B$ has a strong absorption of neutron, unless only $^{11}B$ is used in the synthesis of the compound.

## 4. Conclusions

In conclusion, we have been successful in synthesis of a novel compound $Ba_3InB_9O_{18}$ with the same structure type of $Ba_3MB_9O_{18}$ ($M$ = Sc, Y, Pr–Yb). X-ray excited luminescence measurements showed that the LY of $Ba_3InB_9O_{18}$ powders is about 75% as large as that of BGO powders under the same measurement conditions, and exhibited a broad and intense emission band in the range of 360–500 nm with a maximum at 400 nm. As for the mechanism of the scintillation performances, the structural features and lattice defects should be taken into account. Further investigation of the detailed mechanism will be useful. Considering the chemical stabilization, emission wavelength range and LY of $Ba_3InB_9O_{18}$ together, the

compound can be a good candidate for efficient and fast scintillators used for X-ray detection applications.

## Acknowledgments

This work was financially supported by the National Natural Science Foundation of China (Grant Numbers 50502039 and 50372081), and the International Center for Diffraction Data (ICDD).

## References

[1] D.M. Drake, L.R. Nilsson, J. Faucett, Nucl. Instrum. Methods 188 (1981) 313.
[2] L.L. Nagornaya, V.D. Ryzhikov, U. Ya. Vostretsov, I.A. Tupitsina, S.F. Burachas, W.P. Martynov, K.A. Katrunov, Radiat. Meas. 24 (1995) 375.
[3] A.A. Annenkov, M.V. Korzhik, P. Lecoq, Nucl. Instrum. Methods A 490 (2002) 30.
[4] M. Kobayashi, Y. Usuki, M. Ishii, M. Itoh, M. Nikl, Nucl. Instrum. Methods A 540 (2005) 381.
[5] D.F. Anderson, Nucl. Instrum. Methods A 287 (1990) 606.
[6] M. Tanaka, K. Hara, S. Kim, K. Kondo, H. Takano, M. Kobayashi, H. Ishibashi, K. Kurashige, K. Susa, M. Ishii, Nucl. Instrum. Methods A 404 (1998) 283.
[7] J.P.J. Carney, D.W. Townsend, Radiat. Phys. Chem. 75 (2006) 2182.
[8] A. Yoshikawa, H. Ogino, J.H. Lee, M. Nikl, N. Solovieva, N. Garnier, C. Dujardin, K. Lebbou, C. Pedrini, T. Fukuda, Opt. Mater. 24 (2003) 275.
[9] L.S. Qin, H.Y. Li, S. Lu, D.Z. Ding, G.H. Ren, J. Cryst. Growth 281 (2005) 518.
[10] M. Nikl, J. Pejchal, E. Mihokova, J.A. Mares, H. Ogino, A. Yoshikawa, T. Fukuda, A. Vedda, C. D'Ambrosio, Appl. Phys. Lett. 88 (2006) 141916.
[11] M.K. Ehlert, G.E. Greedan, M.A. Subramanian, J. Solid State Chem. 75 (1988) 188.
[12] M. He, L. Kienle, A. Simon, X.L. Chen, V. Duppel, J. Solid State Chem. 177 (2004) 3212.
[13] L. Wu, X.L. Chen, H. Li, M. He, Y.P. Xu, X.Z. Li, Inorg. Chem. 44 (2005) 409.
[14] L.Y. Li, G.B. Li, Y.X. Wang, F.H. Liao, J.H. Lin, Chem. Mater. 17 (2005) 4174.
[15] F. Kong, S.P. Huang, Z.M. Sun, J.G. Mao, W.D. Chen, J. Am. Chem. Soc. 128 (2006) 7750.
[16] C.J. Duan, W.F. Li, X.Y. Wu, H.H. Chen, X.X. Yang, J.T. Zhao, J. Lumin. 117 (2006) 83.
[17] Z. Yang, X.L. Chen, J.K. Liang, Y.C. Lan, T. Xu, J. Alloy. Compd. 319 (2001) 247.
[18] S.Y. Zhang, L. Wu, X.L. Chen, M. He, Y.G. Cao, Y.T. Song, D.Q. Ni, Mater. Res. Bull. 38 (2003) 783.
[19] Y. Zhang, X.L. Chen, J.K. Liang, T. Xu, J. Alloy. Compd. 348 (2003) 314.
[20] X.Z. Li, C. Wang, X.L. Chen, H. Li, L.S. Jia, L. Wu, Y.X. du, Y.P. Xu, Inorg. Chem. 43 (2004) 8555.
[21] M. He, X.L. Chen, Y.P. Sun, J. Liu, J.T. Zhao, C.J. Duan, Cryst. Growth Des. 7 (2007) 199.
[22] G. Cai, M. He, Y.F. Lou, X.L. Chen, W.Y. Wang, H.H. Chen, J.T. Zhao, Powder Diffr., unpublished results.
[23] J.R. Cox, D.A. Keszler, Acta Crystallogr. C 50 (1994) 1857.
[24] G. Blasse, C. de Mello Donega, I. Berezovskaya, V. Dotsenko, Solid State Commun. 91 (1994) 29.
[25] G. Blasse, C. de Mello Donegá, N. Efryushina, V. Dotsenko, I. Berezovskaya, Solid State Commun. 92 (1994) 687.
[26] P.F. Rza-Zade, F.A. Ismailova, K.L. Ganf, M.I. Safarov, M.Z. Ali-Zade, Inorg. Mater. 15 (1979) 223 (English translation).
[27] K.I. Schaffers, D.A. Keszler, Acta Crystallogr. C 49 (1993) 211.
[28] N. Penin, M. Touboul, G. Nowogrocki, Solid State Sci. 3 (2001) 461.
[29] A. Boultif, D. Louer, J. Appl. Crystallogr. 37 (2004) 724.
[30] S.K. Kurtz, T.T. Perry, J. Appl. Phys. 39 (1968) 3798.
[31] H.M. Rietveld, Acta Crystallogr. 22 (1967) 151.
[32] J. Rodriguez-Carvajal, FullProf (Version 3.5d Oct98-LLB-JRC).
[33] M. Marezio, Acta Crystallogr. 20 (1966) 723.
[34] J.R. Cox, D.A. Keszler, J.F. Huang, Chem. Mater. 6 (1994) 2008.
[35] X.Z. Li, X.L. Chen, J.K. Jian, L. Wu, Y.P. Xu, Y.G. Cao, J. Solid State Chem. 177 (2004) 216.
[36] I.D. Brown, D. Altermatt, Acta Crystallogr. B 41 (1985) 244.
[37] E.I. Kamitsos, M. Karakassides, G.D. Chryssikos, J. Phys. Chem. 91 (1987) 1073.
[38] C.J. Duan, J.L. Yuan, J.T. Zhao, J. Solid State Chem. 178 (2005) 3698.